

Low temperature S-shaped heat capacities in finite nuclei

Osvaldo Civitarese

*Departamento de Física, Universidad Nacional de La Plata,
c.c. 67 1900, La Plata, Argentina*

Peter O. Hess and Jorge G. Hirsch

*Instituto de Ciencias Nucleares, Universidad Nacional Autónoma de México,
Apartado Postal 70-543, 04510 México D.F., Méx.*

Recibido el 17 de marzo de 2004; aceptado el 11 de mayo de 2004

While in the thermodynamic limit a phase transition is signaled by the presence of a sharp peak in the specific heat, in finite systems a bump is usually found. However, there are relevant cases in which the presence of a low-temperature bump in the canonical specific heat of atomic nuclei is linked to the existence of isolated low energy states through a local Schottky effect, and do not represent a phase transition. Examples are presented for light and heavy deformed nuclei, by using in the calculations experimental and theoretical energy levels.

Keywords: Phase transition in nuclei; heat capacities.

En el límite termodinámico una transición de fase está asociada a un pico bien definido en el calor específico. Por otro lado, en sistemas finitos como los núcleos atómicos se encuentran elevaciones anchas en el calor específico que no representan una transformación de fase. Estos aparecen debido a la existencia de niveles aislados de baja energía a través del efecto Schottky local. Se presentan ejemplos de este comportamiento para núcleos deformados pesados y ligeros, y empleando tanto niveles de energía experimentales como espectros calculados en un modelo sencillo.

Descriptores: Transición de fase en núcleos atómicos; calor específico.

PACS: 05.30.Fk, 24.10.Pa, 27.30.+t, 27.70.+q

1. Introduction

The experimental determination of level densities in the 0 - 6 MeV region of the spectrum of some heavy deformed nuclei has allowed the deduction of the entropy, temperature and heat capacity within the microcanonical and canonical ensembles [1]. The heat capacity exhibits an S-shape as a function of temperature, which is interpreted as a fingerprint of a phase transition from a strongly correlated to an uncorrelated phase. Shell model Monte Carlo studies of iron isotopes support the presence of a pairing phase transition [2], which is correlated with the suppression of the number of spin-zero neutron pairs as the temperature increases [3].

The analysis of caloric curves in small systems requires new approaches [4]. Simple models have been used to analyze the pairing phase transition [5]. A gradual transition from strongly paired states to unpaired states in rare earth nuclei at low spin has been found [6]. While the liquid-gas phase transition is characterized at higher temperatures by abnormally large kinetic energy fluctuations [7], at lower temperatures the vanishing of the pairing gap, predicted in the finite temperature BCS formalism [8,9] and taking into account thermal and quantum fluctuations, washed out the sharp phase transition [10].

Different studies have proposed the existence of a shape phase transition, from deformed to spherical, at relatively low temperatures [11, 12]. Attempts were made to link a prominent peak in the specific heat with this shape phase transition [13, 14]. But it was soon realized that the reduction in the expectation value of the quadrupole moment as the tempera-

ture increases does not reflect a true phase transitions, but the mixing of deformed configurations with opposite sign [15]. Also, the existence of the bump in the specific heat is better explained by the finite size of the configuration space [16,17], which imposes an upper limit to the energy accessible at the nucleus, producing the well known Schottky effect [18, 19].

When the specific heat is studied in the canonical ensemble, there is always a first bump at low temperature present, which often has the form of a reclined S, as can be recognized in Figs. 1, 3, 5 and 6. It is found at around $T \approx 0.5$ MeV in light nuclei [13, 15, 17] and at $T \approx 0.1$ MeV in heavy nuclei [1]. Its origin was tentatively associated with the presence of the ground-state rotational band [13].

In the present paper we show, in a model independent way, that the peak in the specific heat at low temperature is a remnant of a Schottky curve, typical of a two-level system [19]. We shall demonstrate that this peak does not disappear when further states are added to the space of configurations. We have applied these concepts to describe the thermal excitation of deformed nuclei within the framework of a simple, albeit realistic, model for rotational states. We have found that the same conclusions can be drawn from these realistic calculations. The emerging mechanism, which explains the appearance of a peaked structure, is the Schottky curve produced by the inversion of the population of the ground state and of the first excited 2^+ state. We have verified the validity of this statement by performing calculation with and without including the first excited quadrupole state in the model space. Care was taken in interpreting the notion of temperature when working within the framework of the

TABLE I. Experimental spectrum of ^{24}Mg . In the first row J_i^π indicate the spin (J), parity (π) and the eigenvalue index (i). In the second row the energies are given in units of MeV.

0_1^+	2_1^+	4_1^+	2_2^+	3_2^+	4_2^+	0_2^+
0.000	1.369	4.123	4.238	5.235	6.010	6.433

quantum statistical mechanics of small systems. Also the notion of phase transition has to be taken with care, because strictly speaking there are no phase transitions in finite systems. Nevertheless, in finite systems a phase transition is associated to rapid changes in thermodynamical quantities like energy and its derivatives [20].

2. Model independent considerations

As a first example we will discuss the case of ^{24}Mg , whose first seven low-lying states are presented in Table I. For the sake of the present discussion we shall not argue about the microscopic structure of the levels but, rather, we shall take the energy and degeneracy of each level as the input of our calculation.

In order to investigate the thermodynamic properties we use the canonical ensemble, with the partition function given by

$$Z(T) = \sum_i \Omega_i e^{-\beta E_i}. \tag{1}$$

The index i runs over all states to be considered, $\Omega_i = 2J_i + 1$ is the degeneracy of the i -th state and E_i is its energy. The quantity $\beta = \frac{1}{T}$ is the inverse temperature and T is the temperature measured in units of MeV (the Boltzmann constant is set to one).

The specific heat

$$C_N = \frac{\partial}{\partial T} \langle E \rangle = \frac{1}{T^2} (\langle E^2 \rangle - \langle E \rangle^2), \tag{2}$$

is calculated from the expectation values of the energy $\langle E \rangle$ and its fluctuations $\langle E^2 \rangle$, where

$$\langle E^n \rangle = \frac{\sum_i \Omega_i E_i^n e^{-\beta E_i}}{Z(T)}. \tag{3}$$

If only the ground state and the first excited 2^+ state are considered, we have the typical case of a two level system, where the lowest level has degeneracy $\Omega_1 = 1$, while the second one has a five fold degeneracy. For this particular system the heat capacity has the temperature dependence plotted with a full line in Fig. 1. As expected, it has the characteristic shape of a Schottky curve [18–20].

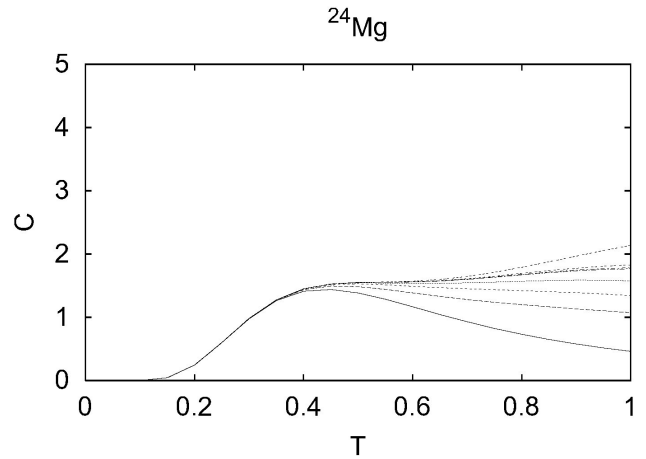


FIGURE 1. Heat capacity of ^{24}Mg . From bottom to top the curves show the results obtained by including the ground state and the first excited state in the partition function (first curve), and then, the results of the calculations after adding one by one all the states of the low-lying spectrum. The curve at the top was obtained by including the first sixteen measured states [21], with their degeneracies.

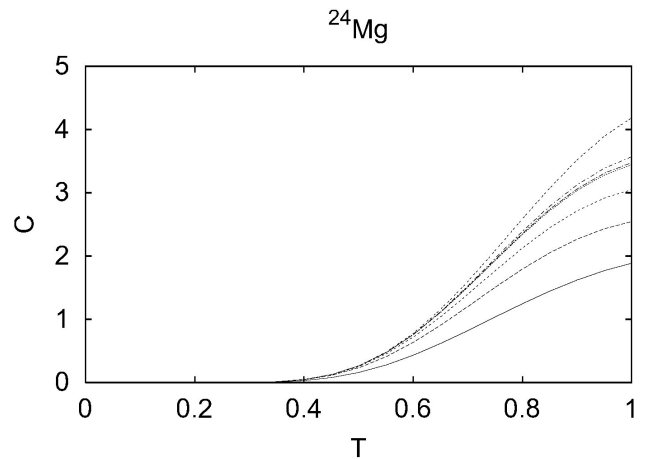


FIGURE 2. Heat capacity for ^{24}Mg . The calculation of the partition function was performed excluding the first excited quadrupole state 2_1^+ , from the sum. The meaning of the curves is the same as in Fig. 1

The other curves of Fig. 1 have been obtained by adding one by one the known states [21] in order of increasing energy, up to the last of the sixteen measured states of the spectrum. It can be seen that the addition of levels to the partition function washes out the peak obtained when only the first two levels are considered, producing an S-shaped structure. The upper curve, which corresponds to the inclusion of the 16 reported levels, exhibits the broad structure typical of the Schottky peak. However, there is a remnant of the peak obtained in the two-level case.

To demonstrate that the low temperature bump in the specific heat is just a remnant of the two-level-like structure, we have proceeded as before, adding gradually more states to the partition function but excluding from the sum the first excited 2^+ state. The results are shown in Fig. 2, where, from bottom to top, the first curve corresponds to the two-level system composed by the ground state and the first excited 4^+

state; and the next curves are obtained by adding one level at a time. The last curve shows the results obtained in the configuration space consisting of the first fifteen observed states of the spectrum, including the ground state and omitting the 2_1^+ state. Now the peak at low energy has disappeared, a clear indication that the bump at low energy is due to the presence of the 2_1^+ state.

Why does the peak of the two-level system $\{0_{g.s.}^+, 2_1^+\}$ survive, through the S-shaped peak? A possible explanation is that at relatively low temperatures the relevant scale is fixed only by the excitation energy of the 2_1^+ state. As the temperature increases the system reacts by increasing the population of the first excited state, while the other states are less likely to influence the partition function due to the large negative values of the exponents βE_i . This produces the Schottky peak at low energy. After the probabilities assigned to the ground state and the first excited state become comparable, the heat capacity saturates and goes down. Another way to describe the situation is that the ground state and the first excited state represent, to a good approximation, an isolated system of two levels which produce a Schottky peak. As the temperature increases the next state (4_1^+) comes into play and the opening of this channel raises the value of the heat capacity again. The contribution to the peak becomes broader, as seen in Fig. 1. The subsequent state (2_2^+) is close in energy to the 4_1^+ state and its contribution makes the peak even broader. The addition of successive states increases the contribution to the heat capacity but is unable to erase the trace left from the first two levels. A similar effect does not happen when the 2_1^+ state is excluded. Although the two-level system composed by the ground state and the 4_1^+ state shows also a Schottky peak, the fact that the following states are in the same energy range eliminates the dominance of the two-level peak.

The same analysis can be performed for a heavy-mass nucleus. As an example we choose ^{168}Er , which is a well deformed nucleus and has rotational bands [21]. The first seven states are listed in Table II. In Fig. 3 we have first considered the two-level system, consisting of the ground state and the first excited 2_1^+ . Then, other states were added, one by one, and finally, we have calculated the heat capacity including the first sixteen experimentally observed states. The results shown in Fig. 4 were obtained by removing the first excited 2_1^+ state from the partition function. Note that slightly below 0.1 MeV a peak appears and the feature above 0.1 MeV indicates a rise in the heat capacity. Whether this feature gives a new peak will be better understood when the schematic model is introduced in Sec. III.

TABLE II. Experimental spectrum of ^{168}Er . Only the first seven low-lying states are shown. The complete spectrum can be obtained from [21]. The values are displayed as in Fig. 1. The energies are given in units of MeV.

0_1^+	2_1^+	4_1^+	6_1^+	2_2^+	3_1^+	8_1^+
0.000	0.080	0.264	0.546	0.821	0.896	0.928

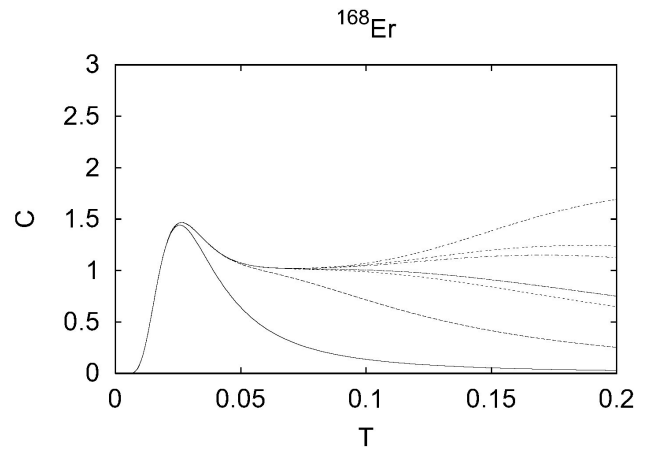


FIGURE 3. Heat capacity for ^{168}Er . From bottom to top, the curves show the results corresponding to: a) the first two levels of the spectrum, b) the gradual addition of levels, and c) the full set of observed states.

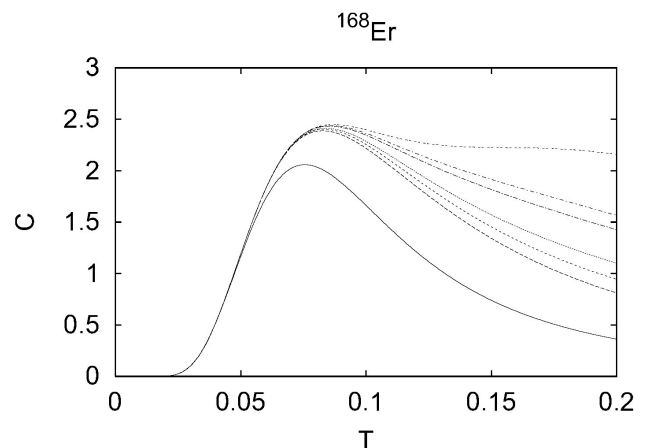


FIGURE 4. Heat capacity for ^{168}Er , calculated with the partition function where the 2_1^+ state is excluded. The explanation is the same as for Fig. 3.

The explanation of the observed features of the heat capacity, calculated with the experimentally observed levels, is the same as the one advanced for the case of ^{24}Mg , namely: the existence of the peak at low temperature is directly related to the presence of the first excited state. When the 2_1^+ state is excluded from the partition function, the peak at low energy disappears (see Fig. 4). In the case of ^{168}Er , the ratio between the energies of the first and higher excited states is smaller than in ^{24}Mg . It reinforces the dominance of the gap between the first excited state and the ground state in determining the energy scale.

3. A simple model

In this section we apply the ideas exposed before to a simple model which allows us to calculate a complete spectrum. We will not explain the model in detail, because the main emphasis of this contribution lies in the thermodynamical properties. The reader can either consult the references given below, or accept the model as a mean to obtain a spectrum.

In this section we calculate the energy spectrum and the partition function, using a collective model which is adequate to the microscopic description of rotational nuclei. It is based on the Elliott $SU(3)$ model [22], which is a suitable model for light-mass nuclei, where the spin-orbit effects are not strong enough to produce the occurrence of states with different principal quantum numbers within a shell. For heavy nuclei the pseudo- $SU(3)$ ($\widetilde{SU}(3)$) [23] will be adopted. In the $\widetilde{SU}(3)$ the orbits (or one body states) of the shell model are divided in normal and unique orbits. The unique orbits are those with the largest angular momentum in a shell. By keeping only the normal orbits and re-defining the spin and angular momentum as the pseudo-spin and pseudo-angular momentum, a new degeneracy of orbits is observed which can be mapped to the scheme of the $\widetilde{SU}(3)$ group. As a first approximation one can deal with heavy nuclei by restricting to normal orbits. The application of an extended version of the model was quite successful, as shown in [24]

The Hamiltonian has in both cases ($SU(3)$ for light and $\widetilde{SU}(3)$ for heavy nuclei) the form:

$$H = \hbar\omega\hat{n} - \frac{\chi}{4}\hat{Q}\cdot\hat{Q} + \alpha\hat{L}^2 + b\hat{K}^2, \quad (4)$$

where \hat{n} is the number operator of excitation quanta, \hat{Q} is the quadrupole operator acting in a single oscillator shell, \hat{L} is the angular momentum operator and \hat{K} gives approximately the projection of the angular momentum onto the intrinsic z-axis. The form of the \hat{K}^2 operator is given in [26]. The energy eigenvalues are given by

$$E = \hbar\omega n - \chi C_2(\lambda, \mu) + aL(L+1) + bK^2. \quad (5)$$

where $C_2(\lambda, \mu) = (\lambda^2 + \lambda\mu + \mu^2 + 3\lambda + 3\mu)$ is the expectation value of the second order Casimir operator of $SU(3)$, (λ, μ) is the $SU(3)$ irreducible representation [25], The value $\hbar\omega$ is fixed as $45A^{-1/3} - 25A^{-2/3}$ MeV for light nuclei, and as $41A^{-1/3}$ MeV for heavy nuclei. The parameter χ is adjusted to the difference of the first excited 0^+ state, the value of $a = \frac{3}{4}\chi + \alpha$ to the energy of the first excited 2^+ state and the value of b to the difference $(E(2_2^+) - E(2_1^+))$. The lowest $SU(3)$ irrep for ^{24}Mg is (8,4) and the next one, which contains a 0^+ state, is (4,6). For ^{168}Er the lowest $\widetilde{SU}(3)$ irrep is (30,8) [24] and the next one with a 0^+ is (32,4). In the calculation, only states with $S = 0$ are considered, which are the most symmetric in their spatial components. Taking into account higher spin states does not significantly modify the results. The shell model space, restricting to $S = 0$ and $\Delta N = 0\hbar\omega$ configurations, is a complete space and the only model dependence is due to the use of the Hamiltonian. The theoretical description of the low energy spectra is, due to the simplicity of the model, not a perfect one, but it is realistic enough for the purpose of the present discussion. The 4_1^+ state of the rotational ground state band is theoretically predicted at 4.56 MeV, compared to the experimental value of 4.12 MeV. The 2_2^+ band-head of the γ -vibrational band, is obtained at about 4.24 MeV. The rest of the spectrum is

in fairly good agreement with data at low energy. Above 6 MeV the model predicts states with spin one, not seen in the experiments. This, of course, limits the validity of the model. However, the main effect on the heat capacity takes place at low energy, where the main contribution comes from states which are well described by the model.

In Table III the adjusted parameters for ^{24}Mg and ^{168}Er are listed.

TABLE III. Parameters of the Hamiltonian, for ^{24}Mg and ^{168}Er .

	$\hbar\omega$	χ	a	b
^{24}Mg	12.6	0.153	0.228	0.717
^{168}Er	7.43	0.029	0.013	0.185

In Fig. 5 the theoretically obtained values of the heat capacity of ^{24}Mg , calculated with the spectrum of the Hamiltonian H , are shown. As in the previous section we have calculated the partition function in different spaces: by including or excluding the first excited 2^+ state. Again, when the 2_1^+ state is excluded the S-shaped peak disappears, in agreement with the discussion in the previous section. The absolute values of the heat capacity agree with those of Figs. 1 and 2.

The same analysis was performed for the case of ^{168}Er and the results are depicted in Fig. 6. The trend of the results and the explanations go along the same line as for the case of ^{24}Mg . The absolute values of the heat capacity also agree with those presented in Sec. II. The peak at low energy, clearly visible with its well defined S-shape structure, disappears when the 2_1^+ state is excluded. However, a peak at a higher temperature appears, which is the contribution from the 4_1^+ state. This is also in agreement with the finding in Fig. 4. The reason for the appearance of the peak is the same as for the 2_1^+ state. The next excited state is still far from the 4_1^+ state and another local Schottky effect appears.

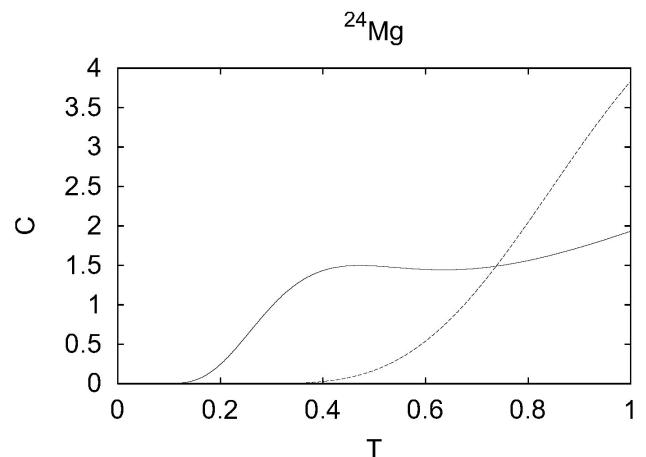


FIGURE 5. Heat capacity of ^{24}Mg within the simple model. The curve with the bump at $T \approx 0.4$ MeV contains all states of $0\hbar\omega$ with $S = 0$. In the other curve the 2_1^+ state was excluded.

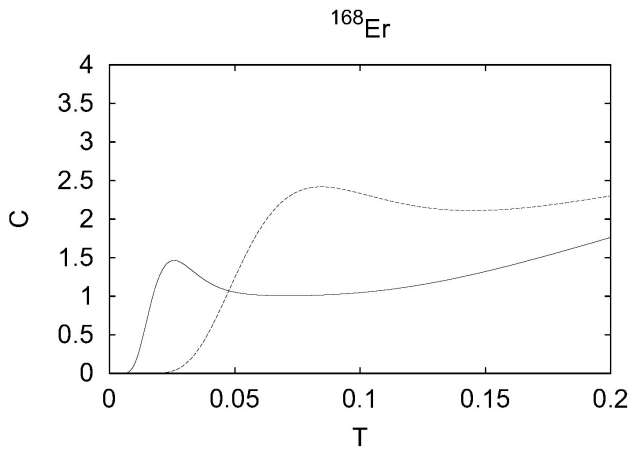


FIGURE 6. Heat capacity of ^{168}Er within the simple model. The curve with the peak at lower temperatures contains all states with $0\hbar\omega$ and $S = 0$, while for the other curve the 2_1^+ state of the ground state rotational band was excluded.

4. Conclusions

A model independent discussion on the specific heat in nuclei at low temperatures was given. It was shown that the bump of the heat capacity at low temperatures, for rotational nuclei, is a remnant of a Schottky effect, *i.e.*: the thermal memory of a two level system situation where the energy difference between the ground state and the first excited state fixes the en-

ergy/temperature scale in a finite size configurational space. In finite systems with discrete spectra, the appearance of a broad Schottky bump is a direct consequence of the finiteness [17, 19], but also the appearance of additional peaks on top of the bump may be due to the discrete nature of the spectrum.

These conclusions are supported by the results of our calculations, based on the use of the $\widetilde{SU}(3)$ model, both for ^{24}Mg and ^{168}Er . The same features were obtained by using phenomenological levels for both cases.

We remind the reader that the systems discussed are finite and, strictly speaking, they cannot undergo a phase transitions. However, phase transitions in finite systems are defined as given by sudden changes in some thermodynamic variables, like the internal energy and its derivatives [20]. The present contribution shows that, using both schematic and realistic examples taken from nuclear structure studies, the existence of peaks in the caloric curve at low energies does not necessarily indicate a phase transition.

Acknowledgments

We acknowledge financial support through the CONACyT-CONICET agreement under the project *Algebraic Methods in Nuclear and Subnuclear Physics*, from CONACyT, and from DGAPA-UNAM project IN119002.

1. E. Melby *et al.*, *Phys. Rev. Lett.* **83** (1999) 3150;
A. Schiller *et al.*, *Phys. Rev. C* **63** (2001) 021306(R);
E. Melby *et al.*, *Phys. Rev. C* **63** (2001) 044309.
2. Y. Alhassid, G.F. Bertsch and L. Fang, *Phys. Rev. C* **68** (2003) 044322.
3. S. Liu and Y. Alhassid, *Phys. Rev. Lett.* **87** (2001) 022501.
4. D.H.E. Gross, *Phys. Rep.* **279** (1997) 119;
A. Schiller, M. Guttormsen, M. Hjorth-Jensen, J. Rekstad and S. Siem, *arXiv:nucl-th/0306082 v1*, (2003).
5. A. Schiller, M. Guttormsen, M. Hjorth-Jensen, J. Rekstad and S. Siem, *Phys. Rev. C* **66** (2002) 024322.
6. A. Belić, D.J. Dean, and M. Hjorth-Jensen, *Nucl. Phys. A* **731** (2004) 381.
7. F. Gulminelli and Ph. Chomaz, *Phys. Rev. Lett.* **82** (1999) 1402;
Ph. Chomaz, V. Duflot, and F. Gulminelli, *Phys. Rev. Lett.* **85** (2000) 3587.
8. A.L. Goodman, *Nucl. Phys. A* **352** (1981) 30.
9. O. Civitarese, G.G. Dussel and R.P.J. Perazzo, *Nucl. Phys. A* **404** (1983) 15.
10. Nguyen Dinh Dang and Nguyen Zuy Thang, *J. Phys. G* **14** (1988) 1471.
11. A.L. Godmann, *Phys. Rev. C* **48** (1993) 2679;
A. L. Goodman, *Phys. Rev. Lett.* **73** (1994) 416;
A. L. Goodman and T. Jin, *Nucl. Phys. A* **611** (1996) 149.
12. G.D. Yen and H.G. Miller, *Phys. Rev. C* **50** (1994) 807.
13. H.G. Miller, R.M. Quick, G. Bozzolo and J.P. Vary, *Phys. Lett. B* **168** (1986) 13;
H.G. Miller, R.M. Quick, and B.J. Cole, *Phys. Rev. C* **39** (1989) 1599;
H.G. Miller, B.J. Cole, and R.M. Quick, *Phys. Rev. Lett.* **63** (1989) 1922.
14. R.K. Bhaduri and W. van Dijk, *Nuc. Phys. A* **485** (1988) 1.
15. J. Dukelsky, A. Poves and J. Retamosa, *Phys. Rev. C* **44** (1991) 2872.
16. O. Civitarese and M. Schvellinger, *J. Phys. G* **20** (1994) 1933, and references therein.
17. O. Civitarese and M. Schvellinger, *Phys. Rev. C* **49** (1994) 1976.
18. R.K. Pathria, *Statistical Mechanics* (Pergamon Press, Oxford, 1978).
19. O. Civitarese, G. G. Dussel and A. Zuker, *Phys. Rev. C* **40** (1989) 2900.
20. W. Greiner, L. Neise and H. Stöcker, *Thermodynamics and Statistical Mechanics*, (Springer, Heidelberg, 1994).
21. C.Y. Cha, N. Nordberg, R.B. Firestone and L.P. Ekström, 1999 ISOTOPE EXPLORER 2.23, Jan. 28;
F. Ajzenberg-Selove, *Nucl. Phys. A* **490** (1988) 1; *ibid.* **506** (1990) 1.

22. J.P. Elliott, *Proc. R. Soc. London, Ser. A* **245** (1958) 128; *ibid.* **245** (1958) 562; M. Harvey, *Adv. Nucl. Phys.* **1** (1968) 67.
23. K.T. Hecht and A. Adler, *Nucl. Phys. A* **137** (1969) 129; A. Arima, M. Harvey and K. Shimizu, *Phys. Lett B* **30** (1969) 517.
24. O. Castaños, P.O. Hess, P. Rocheford and J.P. Draayer, *Nucl. Phys. A* **524** (1991) 469.
25. J.P. Elliott and P.G. Dawber, *Symmetry in Physics: I and II*, (Oxford University Press, Oxford, 1979).
26. H. Naqvi and J.P. Draayer, *Nucl. Phys. A* **516** (1990) 351.